

# Modeling eruptions of Karymsky volcano

A. Ozerov\*, I. Ispolatov†, and J. Lees‡

\*... Russian Academy of Science, Petropavlovsk-Kamchatsky, Russia, †Center for Studies in Physics and Biology, Rockefeller University, New York, NY 10021, ‡Department of Geological Sciences, University of North Carolina Chapel Hill, NC 27599-3315.

A model is proposed to explain temporal patterns of activity in a class of periodically exploding Strombolian-type volcanos. These patterns include major events (explosions) which follow each other every 10-30 minutes and subsequent tremor with a typical period of 1 second. This two-periodic activity is thought to be caused by two distinct mechanisms of accumulation of the elastic energy in the moving magma column: compressibility of the magma in the lower conduit and viscoelastic response of the almost solid magma plug on the top. A release of the elastic energy happens when a stick-slip dynamic phase transition in a boundary layer along the walls of the conduit occurs; this phase transition is driven by the shear stress accumulated in the boundary layer. The first-order character and intrinsic hysteresis of this phase transition explains the long periods of inactivity in the explosion cycle. Temporal characteristics of the model are found to be qualitatively similar to the acoustic and seismic signals recorded at Karymsky volcano in Kamchatka.

Keywords: stick-slip phase transition, viscoelasticity, hysteresis.

## I. INTRODUCTION

A wide variety of types of volcanic activity exists: from devastating explosions separated by calm periods of many years or even centuries to a steady continuous outpouring of magma. In this paper we study mechanisms that give rise to a Strombolian-type volcanic activity, which is somewhere between these two extremes and characterized by regularly repeated explosions (10-400 per day) followed by relatively calm periods. Often in the course of a longer explosion, the gas and ash emission exhibits audible and visible modulations with a rather robust period of about 1 second. These modulations, often found on the seismograms of Strombolian-type eruptions, received a special name, “chugging” (Benoit and McNutt, 1997), because they resemble a periodic noise produced by a steam engine. An example of a volcano exhibiting such activity, we consider Karymsky volcano on Kamchatka peninsula in the Far East of Russia.

We believe that these Strombolian-type eruption patterns are caused by peculiarities of the motion of the magma column, and propose a model that describes the magma motion in a volcanic conduit as a creep flow of viscoelastic compressible medium with shear-stress-dependent boundary conditions. We show that the dynamics of the model indeed exhibits 2 levels of quasiperiodic behavior and resembles the eruption patterns of the Strombolian-type volcanos both on long and short time scales. The physical transparency of the suggested model allows us to express the observed time scales using the material properties of the magma.

Our paper is organized in the following way: first, we briefly describe geological aspects of the current eruption of Karymsky volcano. Then, after referring to the existing explanations of Strombolian-type activity, the model is formally introduced. We derive simple analytical expressions for a dormant time, a duration of explosion, and a typical period of tremor, and then present a numerical solution to a system of dynamical equations describing the motion of the magma column. The paper is concluded with a discussion of results and possible directions for further studies.

## II. THE KARYMSKY ERUPTION OF 1996 - 2000



**Fig. 1.** Karymsky volcano.

Karymsky volcano (Fig. 1), located in the central part of the East Kamchatka volcanic belt, is one of the most active volcanoes in the far-eastern Russia. It is a typical andesite stratovolcano composed of a 7700 – 7800-year old caldera  $\sim 5$  km in diameter (Ivanov et al., 1991) and a more recent cone which started growing about 5300 years ago and at present (September 2000) is  $\sim 700$  m high. The cone is composed of accumulated lava and pyroclastic materials, and the summit of the cone is capped by a double crater. The active part of the crater, formed during the most recent eruption, widened from 90 m in 1996 to 190 m in 2000 (Fig. 2). The absolute height of the volcano is 1549 m.



**Fig. 2.** Double summit crater at Karymsky volcano.

Karymsky activity usually consists of long effusive-explosive eruptions, with the eruption previous to the one being studied taking place in 1970-1982. The current eruption at Karymsky volcano began in January 1996 and apparently entered a lull phase in December 2000. Each eruption consists mostly of the discrete quasiperiodic gas and ash bursts sending plumes 100-1000 m above the crater rim (Fig. 3).



**Fig. 2.** Gas and ash plums at Karymsky volcano.

Ash and steam clouds have been observed extending downwind for 10-50 km, rarely 100-200 km.

A lava flow field, produced by the very viscous magma, runs down the south-western slope of the cone and reaches the length of  $\sim 1.4$  km and the width  $\sim 100 - 200$  m. Even during the periods of highest activity, the motion of the lava flows was very slow (few meters per day) and was noticeable only by periodic rock-falls, happening every 5-15 minutes.

During particularly strong explosions, the eruptive column collapsed causing pyroclastic flows. In the lower part of the eruptive column, hot volcanic bombs of the sizes up to 2, rarely 5 m, were frequently observed. The bombs were dense and often covered with a bread-crust-like structure formed during cooling. On the surface of some bombs, noticeable extrusive tracks were found; they were scratched on the very viscous moving magma by the protruding parts of the magma channel.

Total volumes of pyroclastic and effusive materials deposited on the cone of Karymsky during the eruption of 1996-2000 is estimated to be 0.0274 and 0.0229 km<sup>3</sup>, respectively. Eruptive products, which include magma, volcanic bombs, and ash, predominantly consist of andesite, usually of black and dark grey color. The most common mineral in the eruptive products is plagioclase (20-25 %). Crystals of plagioclase can reach a size of 3-5 mm. The concentration of olivine and pyroxene is less than 1%, their crystal sizes are usually 2-3 mm. A chemical content of the andesite, averaged over 6 samples from the 1996 - 2000 eruption, is listed below:  $SiO_2 - 61.54$ ,  $TiO_2 - 0.86$ ,  $Al_2O_3 - 16.67$ ,  $Fe_2O_3 - 2.43$ ,  $FeO - 5.12$ ,  $MnO - 0.11$ ,  $MgO - 1.99$ ,  $CaO - 5.31$ ,  $Na_2O - 3.69$ ,  $K_2O - 1.58$ ,  $P_2O_5 - 0.25$ .

The feeding system of Karymsky volcano was studied by various methods, including gravity surveys, aeromagnetic surveys, photogrammetry, seismology and geodesy (Zubin, 1971; Maguskin, 1982; Shirokov, 1988). Despite slight discrepancies in the estimates of the depth of the upper border of magma chamber and its size, these data agree that underneath the Karymsky volcano in the close proximity to the surface there exists a spherical magma chamber. The upper border of this chamber is in few kilometers below the sea level. The diameter of the magma chamber is estimated to be between 1.5 and 7 km. A magma channel of a diameter of 100-200 m leads from the magma chamber to the top crater.

### III. DUAL PERIODICITY OF KARYMSKY ERUPTION

A distinctive feature of Karymsky eruptions is its rather robust periodicity which is observed on two timescales. An explosion, and a following quiet period, define the first period of activity which varied between 3 and 20 minutes and sometimes extending up to an hour. An explosion itself can start either abruptly or gradually (Fig. 4) and proceed according to one of the following scenarios:

## Karymsky Acoustic Boom-Chugs

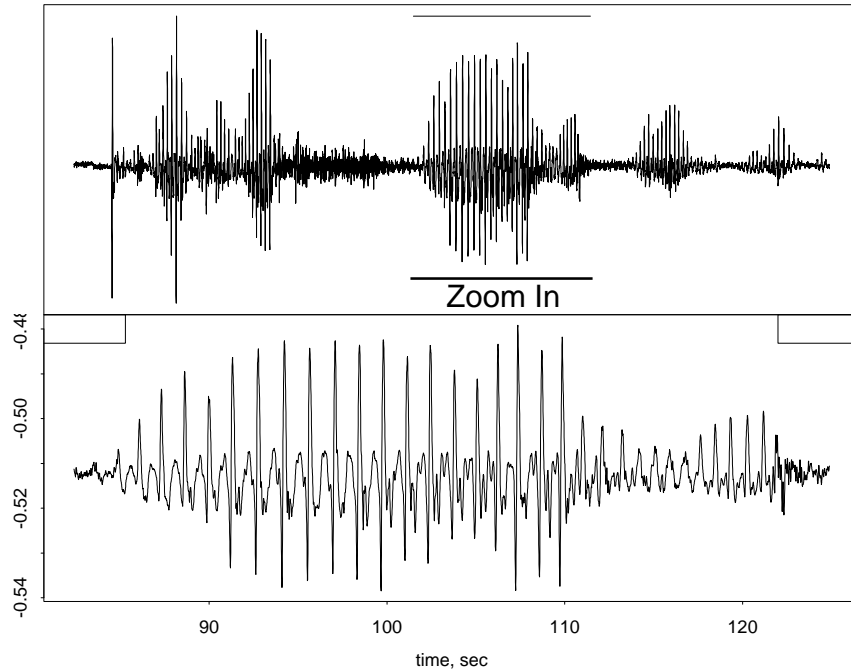


**Fig. 4.** Typical acoustic signal of a period of activity of Karymsky volcano

during shorter explosions, the activity decays quickly and monotonously (in less than 10 seconds), while the longer explosions (20 – 40 s, rarely 1 minute) may contain periods of relatively high and low activity. Often during longer (> 20s) explosions, the intensity of the acoustic and seismic signals emitted by the volcano exhibits chugging, i.e. modulations with a typical period of  $\sim 1$  second. The chugging defines the second, shorter, period in the cyclic activity of the volcano. A typical chugging event consists of 10-20 cycles (Fig. 4). The explosion is followed by a quiet period characterized by a complete lack of any activity in the crater and usually lasting much longer than the explosions themselves. Similar temporal patterns have been also observed during previous Karymsky eruptions. (Tokarev and Firstov, 1967; Farberov et al., 1983).

The systematic seismic and acoustic studies of Karymsky volcano were conducted in 1997-1999 by 3 Russian-US expeditions. The seismograms presented in Fig. 4 were recorded in 1998 by a three-component wide-band seismometers CMG 40-T, but the most detailed information about a fine structure of the chugging signal was obtained using a set of infrasound microphones. For a more complete description of the seismic and infrasound recordings at Karymsky the reader is referred to (Johnson et al., 1998; Johnson, 2000; Johnson and Lees, 2000).

## IV. EXISTING MODELS OF ERUPTION PERIODICITY

Currently there is no single well-established view on the mechanism causing periodic patterns in the eruptions of Strombolian type. Below we mention several possible explanations of origins of the periodicity. Lees and Bolton (1998) compared the eruption process to the steam exhaust from a hydrodynamic system with a nonlinearly controlled exhaust valve resembling a pressure cooker. Manga (1996) suggested that the periodicity is caused by a segregation of ascending bubbles into waves, as in a pint of Guinness beer. Julian (1994) proposed a mechanism of nonlinear hydrodynamic oscillations in the ascending magma flow. Jaupart and Vergnolle (1989) suggested that oscillations are caused by periodical collapse of a bubble foam trapped in pockets of the magma chamber. Recently, there appeared a paper by Delinger and Hoblit (1999) where an *ad hoc* hysteresis model was developed to describe a periodic behavior of silicic volcanoes. However, self-consistent explanation for both long- and short-time periodicity and extended calm periods in the activity of Strombolian-type volcanoes is still missing. Our model, based on viscoelastic hydrodynamical

description of the motion of the magma column with shear stress-dependent boundary conditions, accounts for both timescales.

## V. THE MODEL

Let us first qualitatively discuss the motion of magma in the conduit. Since the temperature and pressure in the magma column decrease with the height, the viscosity of magma increases rapidly in the upper part of the conduit. Inspecting eruption products ejected to the surface, it is natural to deduce that at the very top of the column the magma is almost solid. However, deeper parts of the magma column are still hot and much less viscous. Given this significant difference in rheological properties of the upper and lower sections of the magma column, we consider the moving magma as consisting of two distinct parts: long lower part (LP) and short upper part (UP). We assume that the viscosity of the magma in the LP is negligible. Due to the large amount of dissolved gases, magma in the LP is compressible. We also assume that there is a constant supply of fresh magma to the bottom of the LP. Unlike the LP, magma in the UP is cold and viscous; in addition to that, as any media near the liquid-solid transition point, it possesses a certain degree of elasticity. Because of the small length of the UP compared to the LP ( $\sim 100$  m vs.  $\sim 5$  km), we can neglect compressibility of the UP. In summary, we consider a long cylindrical tube filled with a non-viscous compressible media, fed to the bottom with a constant velocity and a short viscoelastic plug (UP) on the top. The boundary conditions for the moving UP are controlled by a local value of a shear stress in the vicinity of the cylinder wall. When the boundary shear stress is low, the plug “sticks” to the cylinder wall and the boundary velocity is zero. As the shear stress increases, the magma near the wall undergoes phase transition (melts) to a much less viscous liquid state, and the boundary layer of the plug slips along the walls of the channel. This shear-induced phase transition happens when the viscoelastic state with the non-zero shear modulus becomes thermodynamically less stable than a pure liquid state with zero shear modulus. Phenomenologically, the transition between stick and slip boundary conditions for the very viscous body is similar to the effect of dry friction, where a motion begins only when a driving force exceeds some threshold value (Persson, 1999, Ch. 8).

Qualitatively, a cycle of the system evolution can be described as follows: when the pressure in the compressible LP of the column is low, the shear stress  $\sigma$  in the plug is much smaller than the threshold phase transition value  $\sigma_{slip}$ , and the velocity of the UP is much less than the feeding velocity  $V_0$ . The difference in feeding and plug velocities results in the growth of the pressure of the compressible magma in LP which, in its turn, increases the shear stress in the plug. This stage corresponds to the dormant period between explosions. When the shear stress in the boundary layer of the UP exceeds the critical value  $\sigma_{slip}$ , the stick-slip phase transition occurs and the plug begins to move. This corresponds to the appearance of visible signs of a volcanic explosion.

Depending on the parameters of the model, the further evolution of the system proceeds according to one of the following two scenarios. For certain conditions, a relaxation of the accumulated in the UP viscoelastic deformations can result in a low, or even reverse, velocity of the boundary layers of the UP relative to the walls of the conduit. If these conditions persist for sufficient time, they can cause a drop of the shear stress below the slip-stick transition critical value  $\sigma_{stick}$ , which in turn can give rise to the reverse, slip-stick transition. However, the stick state will be very short-lived, since the accumulated excessive pressure in the LP and oscillatory motion of UP will result in the immediate increase of the boundary shear stress and a new stick-slip transition. Length of a period of such coupled viscoelastic-stick-slip process is controlled by the density, the elastic modulus, and the characteristic time of the phase transition. In the second scenario, sticking does not occur during short-periodic viscoelastic oscillations of the UP, and the period of these oscillations is roughly equal to that of a freely oscillating elastic membrane with mixed boundary conditions. Either of these oscillation processes can cause the short-period modulation of the activity of the volcano.

During the active phase, the velocity of the UP is much higher than the feeding velocity  $V_0$  which results in an expansion of the LP and a decrease of pressure under the UP. When the pressure under the UP drops so that the shear stress in the UP is below the slip-stick threshold value  $\sigma_{stick}$ , a “long-term” sticking of the plug occurs, and the system enters a new quiet period of evolution. Because of the hysteresis ( $\sigma_{slip} < \sigma_{stick}$ ) associated with the first order nature of the stick-slip transition, it takes some time to build enough pressure for a new explosion to begin. This cycle corresponds to the second, longer period (10-30 minutes) in the dynamics of eruption.

Although simple in nature, this model qualitatively explains both scales of periodicity of Karymsky volcano and does not contradict to the observations. Below a formal analysis of the dynamics of the model is presented.

Let us consider a cylinder (LP) of the radius  $R$  and the length  $L$ , filled with an ideal non-viscous compressible medium fed from the bottom with a constant velocity  $V_0$ . The top of LP ends with a short viscoelastic plug (UP) of length  $l$ ,  $l \ll L$  (Fig. 5).

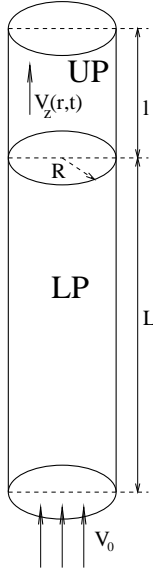


**Fig. 5.** Sketch of the magma conduit.

The velocity field in the UP, of density  $\rho$  and driven by pressure  $P$  and stress tensor  $\sigma_{ij}$ , is described by the Navier-Stokes equation,

$$\rho \frac{\partial v_j}{\partial t} = -\frac{\partial P}{\partial x_j} + \frac{\partial \sigma_{ij}}{\partial x_i}. \quad (1)$$

Because of the high viscosity and the low velocity of magma in the UP, the nonlinear (convective) term is omitted. To account for the viscoelastic properties of the UP we use the simple linear Maxwell model (see, for example, Shore et al.), with a characteristic memory time  $\tau_m$ ,

$$\tau_m \frac{\partial \sigma_{ij}}{\partial t} = -\sigma_{ij} + \eta e_{ij}. \quad (2)$$

Here  $\eta$  is the dynamic viscosity, and  $e_{ij} \equiv \partial v_i / \partial x_j + \partial v_j / \partial x_i$  is the shear rate tensor. Incompressibility condition for the magma in the UP reads:

$$\frac{\partial v_i}{\partial x_i} = 0. \quad (3)$$

For simplicity, we assume that the motion of the plug is axially symmetric and select the  $Z$  direction of our cylindrical coordinate system parallel the axis of the cylinder directed along the magma flow. Also, we also consider the pressure gradient constant through the UP and being equal to  $-\frac{P_0}{l}$ , where  $P_0$  is a pressure at the bottom of the UP. Using (2,3), the Navier-Stokes equation (1) for  $V_z$  ( $Z$ -component of the velocity of the plug averaged over the plug length) can be transformed to:

$$\rho \frac{\partial V_z(r, t)}{\partial t} = \frac{P_0(t)}{l} + \frac{\eta}{\tau_m} \int^t \exp\left(-\frac{t-t'}{\tau_m}\right) \Delta_r V_z(r, t') dt'. \quad (4)$$

Here  $\Delta_r \equiv \partial^2 / \partial r^2 + 1/r \partial / \partial r$  is the radial part of the Laplacian operator in the cylindrical coordinates.

From the conservation of mass of the compressible media in the LP, it follows for the pressure  $P_0$  on the bottom surface of the UP,

$$V(t) - V_0 = -\beta L \frac{dP_0(t)}{dt}, \quad V(t) \equiv 2 \int_0^R V_z(r, t) r dr / R^2, \quad (5)$$

where  $\beta \equiv -1/v(\partial v / \partial p)_T$  is the compressibility (isothermal) of the media in the LP, and  $V(t)$  is the velocity of the UP  $V_z(r, t)$ , averaged over the perpendicular crosssection.

To complete the description of the dynamics of the system, the equations (4,5) must be complemented by boundary conditions for the velocity on the conduit walls,  $V_z(r = R, t)$ . These boundary conditions are controlled by the kinetics

of the first-order phase transition driven by the value of the shear stress  $\bar{\sigma}(t) \equiv \sigma_{rz}(t, R)$  near the wall and are written in a general mixed form:

$$V_z(R, t) = -R\psi(t) \left. \frac{\partial V_z(r, t)}{\partial r} \right|_{r=R}. \quad (6)$$

The quantity  $R\psi(t)$  is usually called a “slipping length”. It shows at what distance inside the wall the linearly extrapolated velocity becomes equal to zero. For  $\psi(t) = 0$  the boundary conditions for the velocity are “stick”, i.e.  $V_z(R, t) = 0$ ; for  $\psi(t) > 0$  the boundary layers of the UP “slip” along the walls of the cylinder with some finite velocity,  $V_z(R, t) > 0$ .

The time evolution of the dimensionless slipping length  $\psi(t)$  is determined from the time-dependent Ginzburg-Landau equation, which describes relaxation of a system with a first-order phase transition:

$$\tau_{GL} \frac{d\psi}{dt} = -\frac{dF}{d\psi}, \quad (7)$$

where  $\tau_{GL}$  sets a phase transition timescale. The free energy  $F(\psi)$  is a usual double-well potential with a tilt depending on the value of the shear stress  $\bar{\sigma}(t)$  on the boundary of the UP. We choose a double-parabola potential which has fixed positions of both minima,  $\psi = 0$  and  $\psi = \psi_0$ :

$$F(\psi) = \begin{cases} \psi^2, & \psi < \psi' \\ (\psi - \psi_0)^2 - h, & \psi \geq \psi' \end{cases} \quad (8)$$

Here  $h$  is a tilt parameter; matching point  $\psi'$  is determined from continuity requirement,  $\psi' = (\psi_0^2 - h)/2\psi_0$ . To determine  $h$  and to illustrate how Eqs. (7,8) work, let us consider a typical stick-slip cycle. We go around a hysteresis curve shown in Fig. 6.

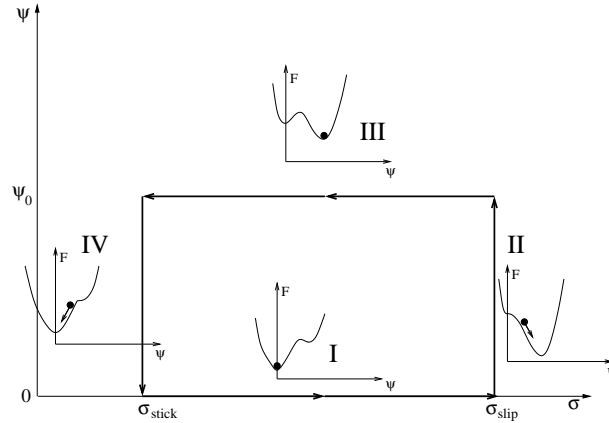


**Fig. 6.** Hysteresis curve **I-II-III-IV** for the stick-slip and the slip-stick transitions. Inserts show typical sketches of  $F(\psi)$  for all branches of the curve.

When the shear stress  $\bar{\sigma}(t)$  is small and growing (line **I**), the boundary condition is “stick” and stationary,  $\psi = \frac{dF}{d\psi} = 0$ . As the shear stress exceeds the critical value  $\sigma_{slip}$ ,  $\psi(t)$  starts moving towards  $\psi_0$  with the rate  $\sim 2\psi_0/\tau_{GL}$  (line **II**). After  $\psi$  reaches  $\psi_0$ , the boundary condition becomes “slip” and stationary again, and the shear stress starts decaying (line **III**). After  $\bar{\sigma}(t)$  drops below  $\sigma_{stick}$ ,  $\psi$  relaxes to 0 (line **IV**). The state **I** corresponds to the dormant period, the state **III** corresponds to the explosion without intermediate sticking; the transition intervals **II**, **IV** are usually very short. The free energy tilt parameter  $h$  is linearly connected to  $\bar{\sigma}$ :

$$h = \psi_0^2 \left[ \frac{2\bar{\sigma}}{\sigma_{slip} - \sigma_{stick}} - \frac{\sigma_{slip} + \sigma_{stick}}{\sigma_{slip} - \sigma_{stick}} \right]. \quad (9)$$

Similarly to the Eq. (4), in the framework of the Maxwell model the shear stress  $\bar{\sigma}(t)$  is expressed as a convolution of a shear rate  $\frac{\partial V_z(r, t')}{\partial r}$  with an exponential memory function  $\exp(-\frac{t-t'}{\tau_m})$

$$\bar{\sigma}(t) = \frac{\eta}{\tau_m} \int^t \exp(-\frac{t-t'}{\tau_m}) \left. \frac{\partial V_z(r, t')}{\partial r} \right|_{r=R} dt' \quad (10)$$

The equations (4–10) completely define the dynamics of our model. A very similar set of equation was derived by Shore et al. (1997) for the physically equivalent model of polymer extrusion. Because of the strong non-linearity of the Eq. (7), an analytic solution of these equations is impossible. We refer readers to Shore et al., 1997, for a detailed description of a linear stability analysis of this system. Contrary to a stable flow, a dynamical regime corresponding to volcanic activity is strongly unstable and nonlinear. However, large separation of characteristic timescales allows us to give reasonable analytical estimates of important temporal features of the model.

Let us first look at the shortest timescale which corresponds to small oscillations of the UP when it slips along the conduit walls without intermediate sticking. For this timescale the pressure term in (4) is considered to be constant. Dynamics of the UP is physically equivalent to the oscillation of an elastic circle membrane with the mixed boundary conditions (6). Only the lowest harmonic is considered,

$$V_z(r, t) = V_0 e^{-i\omega t} J_0\left(\frac{r}{R}\lambda\right), \quad (11)$$

where  $\lambda$ , a number of order of one, depends on the slipping length  $\psi$ :  $J_0(\lambda) = J_1(\lambda)\lambda\psi$ . Here  $J_0$  and  $J_1$  are the zero- and first-order Bessel functions. After plugging Eq. (11) into Eq. (4) and disregarding the constant pressure term, we obtain the following dispersion relation:

$$\omega = \frac{-i \pm \sqrt{4\frac{\lambda^2 \eta \tau_m}{R^2 \rho} - 1}}{2\tau_m}. \quad (12)$$

This yields for a period  $T_{osc}$  of not too overdamped UP oscillations ( $T_{osc} \gg \tau_m$ ):

$$T_{osc} \approx \frac{2\pi R}{\lambda} \sqrt{\frac{\rho \tau_m}{\eta}}. \quad (13)$$

Taking into account a commonly used relation between the Maxwell time and shear modulus  $G$ ,  $\tau_m \approx \eta/G$  (see, for example, Webb (1997)), we observe that Eq. (13) reduces to a usual expressions for a period of a small free oscillations of an elastic membrane,

$$T_{osc} \approx \frac{2\pi R}{\lambda} \sqrt{\frac{\rho}{G}}. \quad (14)$$

Now we go to much longer timescales,  $T \gg \{T_{osc}, \tau_m\}$  and look first at the steady state UP boundary shear stress  $\bar{\sigma} = \left. \frac{\partial V_z(r)}{\partial r} \right|_{r=R}$ . Since this timescale is much greater than the elastic memory time  $\tau_m$ , the viscoelastic term in (4) is relaxed to a usual viscous term,  $\eta \Delta_r V_z(r, t)$ . For a steady state, the averaged over the crosssection of the conduit velocity  $V(t)$  must be equal to  $V_0$ . For an arbitrary slipping length  $\psi$ , a straightforward calculation yields:

$$\bar{\sigma} = \frac{4V_0\eta}{R} \frac{1}{1+4\psi}. \quad (15)$$

It immediately follows that in order for stick-slip repeating cycles to happen, the “stick” steady state shear stress ( $\bar{\sigma}$  for  $\psi = 0$ ) should be greater than  $\sigma_{slip}$  and “slip” steady state shear stress ( $\bar{\sigma}$  for  $\psi = \psi_0$ ) should be less than  $\sigma_{stick}$ . These conditions imply for the feeding velocity  $V_0$ :

$$\frac{\sigma_{slip}R}{4} < V_0 < \frac{\sigma_{stick}R(1+4\psi_0)}{4}. \quad (16)$$

Besides the steady state properties, we can also evaluate characteristic times between the stick-slip and the slip-stick phase transitions, i.e. duration of the dormant and explosive periods. Assuming that these times are much longer than both  $T_{osc}$  and  $\tau_m$ , we again disregard all memory effects in the viscous term in Eq. (4) and consider the flow inertialess by omitting the left-hand-side term  $\frac{\partial V_z(r, t)}{\partial t}$ . After averaging the remaining part of Eq. (4) over the crosssection of the flow and plugging it in (5), we obtain for arbitrary slipping length  $\psi$ :

$$\int^t \frac{V_0 - V(t')}{\beta Ll} dt' - \frac{8\eta V(t)}{R^2(1+4\psi)} = 0. \quad (17)$$

Combining the solution of this equation,



$$V(t) = V_o + C e^{-\frac{t}{t_0}}, \quad t_0 \equiv \frac{8\eta\beta Ll}{R^2(1+4\psi)}, \quad (18)$$

with expressions for stick and slip velocity that follow from (15), we obtain for dormant ( $T_d$ ) and explosive ( $T_e$ ) times:

$$T_d = \frac{8\eta\beta Ll}{R^2} \ln \frac{4\eta V_0 - \sigma_{stick} R}{4\eta V_0 - \sigma_{slip} R} \quad (19)$$

$$T_e = \frac{8\eta\beta Ll}{R^2(1+4\psi_0)} \ln \frac{\sigma_{slip} R(1+4\psi_0) - 4\eta V_0}{\sigma_{stick} R(1+4\psi_0) - 4\eta V_0}. \quad (20)$$

## VI. NUMERICAL RESULTS

To check our analytical predictions and get an overall view of the system dynamics, we solved the Eqs. (4–10) numerically. We used a simple Eulerian finite-difference scheme with a uniform radial grid of 50-100 points. All the integrals are approximated by trapezoid formula. Given that time step is sufficiently small to avoid von Neumann-type instabilities, this simplest difference scheme proved to be sufficiently robust.

We chose the numerical parameters to be in general accordance with the literature (Murase and McBirney, 1973; Borgia and Linneman, 1990; Griffiths and Fink, 1993; Bagdassarov and Dorfman, 1994; Webb, 1997; Bagdassarov and Dorfman, 1998) and with our estimates (14,16,19,20). The following values were used:

Density  $\rho = 2400 \text{ kg/m}^3$

Dynamic viscosity  $\eta = 10^9 \text{ Pa s}$

Conduit radius  $R = 50 \text{ m}$

UP length  $l = 100 \text{ m}$

LP length  $L = 5 \text{ km}$

Compressibility  $\beta = 4 \cdot 10^{-10} \text{ Pa}^{-1}$

Maxwell time  $\tau_m = 0.4 \text{ s}$

Ginzburg-Landau time  $\tau_{GL} = 10^{-3} \text{ s}$

Average velocity  $V_0 = 2 \times 10^{-3} \text{ m/s}$

Slipping shear stress  $\sigma_{slip} = 10^5 \text{ Pa}$

Sticking shear stress  $\sigma_{stick} = 3 \cdot 10^4 \text{ Pa}$

Dimensionless slipping length  $\psi = 10$

With this choice of numerical parameters a no-stick explosion takes place, during which the UP moves along the walls of the conduit with the constant slipping length  $\psi R$  until it finally sticks to the wall at the end of the explosion. For such explosions a choice of phase transition time  $\tau_{GL}$  does not affect the dynamics, given that it is shorter than explosion time,  $\tau_{GL} \ll T_e$ .

Plots of averaged over crosssection velocity  $V(t)$  and pressure gradient vs. time are presented in Fig. 7. The simulation results for dormant and explosion times, as well for short-term oscillation period,  $T_d^s \approx 530 \text{ s}$ ,  $T_e^s \approx 21 \text{ s}$ ,  $T_{osc}^s \approx 0.69 \text{ s}$  are in good agreement with our simple analytical estimates,  $T_d = 497 \text{ s}$ ,  $T_e = 20 \text{ s}$ , and  $T_{osc} = 0.69 \text{ s}$ . To calculate  $T_{osc}$  we have to solve the equation  $J_0(\lambda) = J_1(\lambda)\lambda\psi$ , which for  $\psi = 10$  yields  $\lambda \approx 0.43$ . For the stick boundary conditions ( $\psi = 0$ ),  $\lambda \approx 2.3$ ; which gives for the period of oscillations at the end of explosion cycle when UP sticks to the walls  $T'_{osc} \approx 0.13$ , which is again in very good agreement with the simulation data.

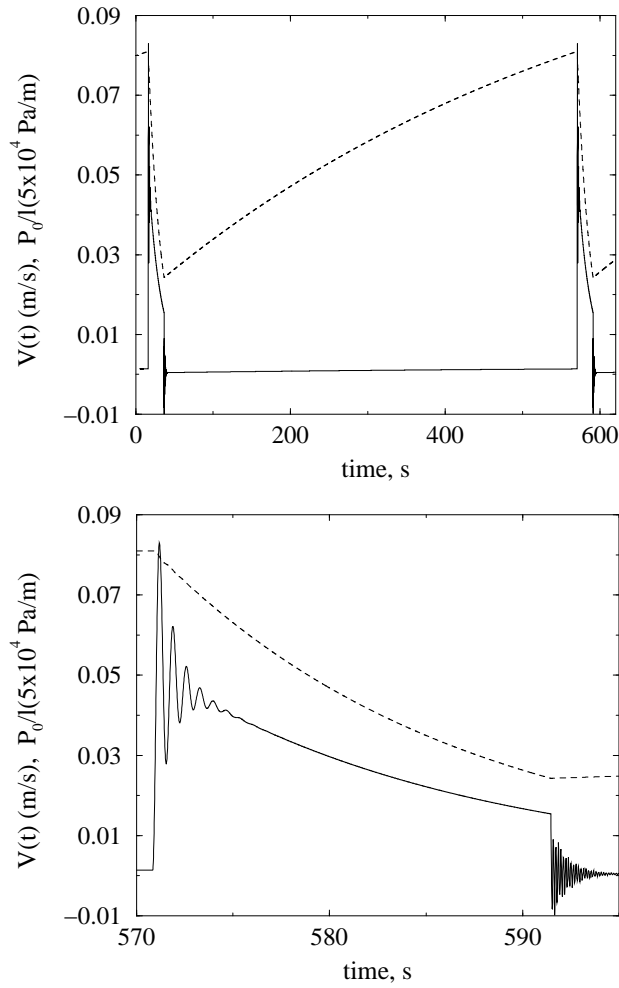


**Fig. 7.** Time dependence of the spatially averaged UP velocity (solid line) and the rescaled pressure gradient (in  $5 \times 10^4$  Pa/m, dashed line).

Another possible scenario for an eruption is when during explosion cycle the UP sticks to the walls numerous times. It happens when the shear stress at the wall, modulated by the free membrane-like oscillations of the UP, drops below the sticking value  $\sigma_{stick}$ , and the slip-stick phase transition is sufficiently fast,  $\tau_{GL} \ll T_{osc}$ . To simulate this regime, we increase the value of  $\sigma_{stick}$  from  $3 \cdot 10^4$  to  $8.5 \cdot 10^4$  Pa and keep all other parameters constant. The long-time dynamics, characterised by the times  $T_e$  and  $T_d$  only slightly changes since both of these times depend on  $\sigma_{stick}$  logarithmically. However, a short-time dynamics, previously described by decaying free oscillations with a period  $T_{osc}$ , changes radically and becomes chaotic (Fig. 8).

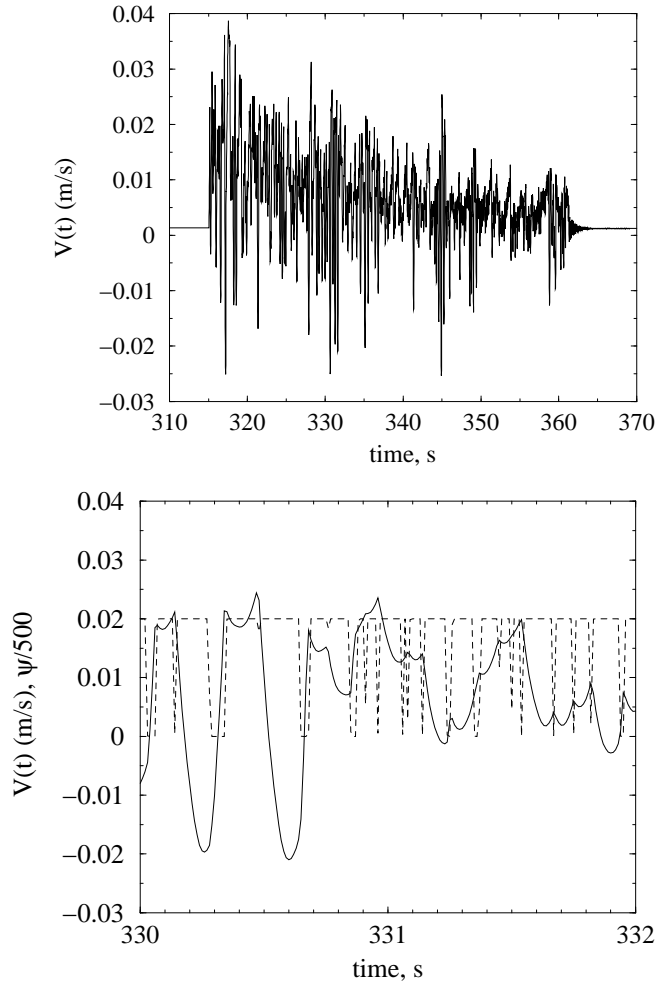


**Fig. 8.** Time dependence of the spatially averaged UP velocity  $V(t)$  (solid line) and the rescaled dimensionless slipping length  $\psi(t)/500$  (dashed line).

A typical time separation between consecutive velocity maxima ( $\approx 0.3$  s for the first three maxima in the bottom part of Fig. 8) becomes somewhat smaller than free oscillation period  $T_{osc} \approx 0.7$ . Qualitatively, it happens when during an oscillation the velocity increases so that shear stress drops below  $\sigma_{stick}$ , a sticking occurs that results in a rapid decrease of velocity, so the oscillation is “truncated” before it reaches its maximum. Another distinct feature of this regime is that the short-time chaotic modulation of the UP velocity continues through the whole explosion phase, while in the non-sticking regime, the oscillations decay after a few periods.

## VII. DISCUSSION

In the previous sections the long-term behavior and two possible scenarios of the short-time activity of the model based on viscoelastic hydrodynamics and stick-slip transition were described. Patterns in the time dependence of the UP velocity, presented in Figs. 7,8, qualitatively match the seismic and acoustic signals (Fig. 4) recorded at Karymsky volcano. Yet nothing has been said about a mechanism describing generation of seismic and acoustic waves themselves. The oscillating UP and related pressure oscillations in the LP can cause seismic waves either directly or act as a “pacemaker” for other processes. These processes can include a stimulated emission of gases either through creation and change of geometry of cracks in the UP or via degassing of magma under action of standing and running compression waves. Since these mechanisms have a strongly nonlinear character, their coupling to the UP oscillation can modify the oscillation period and decay patterns. We leave consideration of these phenomena for future study.

## VIII. CONCLUSION

As a result of the visual, seismic, and acoustic observations at Karymsky volcano, two scales of temporal periodicity were observed in the eruptive dynamics. First, the repetitive explosions which produced the ash and gas clouds and volcanic bombs in 10-20 minutes intervals, and secondly, the periodic modulation of eruptive activity (chugging) with a typical timescale of order of 1 s. The existence of these two scales of temporal periodicity are not limited to the 1996-2000 eruption of Karymsky volcano, similar timescales were observed during previous Karymsky eruptions and on other andesite volcanos in the world.

A model of the motion of the magma column was suggested that accounts for both timescales in the eruption of Karymsky and other similar andesite Strombolian-type volcanos. Low- and high-frequency periodicity is caused by two distinct ways of accumulation of the elastic energy. The viscoelastic properties of the UP causes the high frequency tremor, while the compressibility of magma in the LP explains the low frequency cycles. The shear-stress-dependent stick-slip phase transition in the UP introduces the hysteresis into the dynamics of the magma column motion and explains the unharmonicity of the oscillations and long dormant periods in the eruption dynamics. Physical simplicity of the model allows analytic estimates for the long and short periods of the explosive activity to be obtained.

## IX. ACKNOWLEDGMENTS

The authors are grateful to Martin Grant for stimulating discussions on the polymer extrusion problem, to Julie M. Kneller for carefully reading the manuscript, and especially to Emily Brodsky for providing important references, numerical values for magma parameters, and carefully reading the manuscript. This work was partially supported by the U.S. National Science Foundation.

## X. BIBLIOGRAPHY

- Bagdassarov N. S., Dingwell D. B. and Webb S. L., 1994. *Viscoelasticity of crystal- and bubble-bearing rhyolite melts*, Phys. Earth Planet. Inter., 83: 83-99.
- Bagdassarov N. and A. Dorfman A., 1998. *Viscoelastic behavior of partially molten granites*, Tectonophysics, 290: 27-45.
- Benoit J. P., McNutt S. R., 1997. *New constraints on source of volcanic tremor at Arsenal Volcano, Costa Rica, using broadband seismic data*. Geoph. Res. Lett., 24: 449-452.
- Bird R. B., Armstrong R. C., and Hassager O., 1987. *Dynamics of Polymeric Liquids*. Vol.1: Fluid mechanics, Wiley, New York.
- Borgia A. and Linneman S. R., 1990. *On the Mechanism of Lava Flow Emplacement and Volcano Growth: Arenal, Costa Rica*. Lava Flows and Domes, ed. J.H. Fink, Springer-Verlag.
- Delinger R. P. and Hoblitt R. P., 1999. *Cyclic eruptive behavior of silicic volcanoes*. Geology, 27: 459-462.
- Farberov A. I., Strocheus A. B., and Pribulov E. S., 1983. *Studies of weak seismicity of Karymsky volcano, August 1978*. Vulkanologija i Seismologija, 3: 78-89 (in Russian).
- Griffiths R. W. and J. H. Fink, 1993. *Effects of surface cooling on the spreading of lava flows and domes*. J. Fluid Mech., 252: 667-702.
- Hess P. S., 1989. *Origins of Igneous Rocks*, Harvard Univ. Press., Cambridge, USA.
- Jaupart C. and Vergnolle S., 1989. *The generation and collapse of a foam layer at the roof of a basaltic magma chamber*. J. Fluid Mech., 203: 347-380.
- Johnson J. B., 2000. *Interpretation of infrasound generated by erupting volcanoes and seismological energy partitioning during Strombolian Explosions*. PhD Thesis, Univ. of Washington, Seattle.
- Johnson J. B. and Lees J. M., 2000. *Plugs and Chugs - Strombolian activity at Karymsky, Russia, and Sangay, Ecuador*. J. Volc. Geotherm. Res., 101: 67-82.
- Johnson J. B., Lees J. M., and Gordeev E. I., 1998. *Degassing explosions at Karymsky volcano, Kamchatka*. Geophys. Res. Lett., 25: 3999-4000.
- Julian B. R., 1994. *Volcanic tremor: Nonlinear excitation by fluid flow*. J. Geoph. Res., 99: 11859-11877.

- Lees J. M. and Bolton E. M., 1998. *Pressure cookers as volcano analogues*. EOS, Trans. Am. Geoph. Un., 79 (45), Fall Meeting Supp., F620.
- Magus'kin M. A., Enman V. B., Seleznev B. V., and Shkred V. I., 1982. *Peculiarities of the Earth core displacement on Karymsky volcano in 1970-1981 from geodesical and photogrammetric data*. Vulkanologija i Seismologija, 4: 49-64 (in Russian).
- Manga M. 1996. *Waves of bubbles in basaltic magmas and lavas*. J. Geoph. Res., 101: 17457-17465.
- Murase T. and McBirney A. R., 1973. *Properties of some common igneous rocks and their melts at high temperatures*, Geol. Soc. Am. Bull., 84: 3563-3592.
- Persson B. N. J. , 1999. *Sliding Friction*. Springer-Verlag, Ch. 8.
- Shirokov V. A., Ivanov V. V., Stepanov V. V., 1988. *On the deep structure of Karymsky volcano and peculiarities of its seismicity: local seismic network data*. Vulkanologija i Seismologija, 3: 71-80 (in Russian).
- Shore J. D. , Ronis D., Piche L., and Grant M., 1997. *Theory of melt instabilities in the capillary flow of polymer melts*. Phys. Rev. E, 55: 2976-2992.
- Tokarev P. I. and Firstov P. P., 1967. *Seismological studies of Karymsky volcano*. Bulluten' Vulkanologicheskikh Stanciy, 43: 9-22 (in Russian).
- Webb S., 1997. *Silicate melts: Relaxation, Rheology, and the Glass transition*. Rev. of Geophys., 35: 191-218.
- Zubin M. I, Ivanov B. V., Shteinberg G. S., 1971. *Structure of Karymsky volcano, Kamchatka, and some aspects of caldera genesis*. Geologiya i Geofizika, 1: 73-81 (in Russian).